

Teleporting independent qubits through a 97 km free-space channel

Juan Yin,^{1,*} He Lu,^{1,*} Ji-Gang Ren,^{1,*} Yuan Cao,¹ Hai-Lin Yong,¹ Yu-Ping Wu,¹ Chang Liu,¹ Sheng-Kai Liao,¹ Yan Jiang,¹ Xin-Dong Cai,¹ Ping Xu,¹

Ge-Sheng Pan,¹ Jian-Yu Wang,² Yu-Ao Chen,¹ Cheng-Zhi Peng,¹ and Jian-Wei Pan¹

¹*Shanghai Branch, National Laboratory for Physical Sciences at Microscale and Department of Modern Physics, University of Science and Technology of China, Shanghai 201315, China*

²*Shanghai Institute of Technical Physics, Chinese Academy of Sciences, Shanghai 200083 China*
(Dated: May 10, 2012)

With the help of quantum entanglement, quantum communication can be achieved between arbitrarily distant places without passing through intermediate locations by quantum teleportation [1]. In the laboratory, quantum teleportation has been demonstrated over short distance by photonic [2, 3] and atomic [4, 5] qubits. Using fiber links, quantum teleportation has been achieved over kilometer distances [6, 7]. Long distance quantum teleportation is of particular interest and has been one of the holy grails of practical quantum communication. Most recently, quantum teleportation over 16 km free-space link was demonstrated [8]. However, a major restriction in this experiment is that the unknown quantum state cannot directly come from outside. Here, based on an ultra-bright multi-photon entanglement source [9], we demonstrate quantum teleportation, closely following the original scheme [1, 2], for any unknown state created outside, between two optical free-space links separated by 97 km. Over a 35-53 dB high-loss quantum channel, an average fidelity of 80.4(9) % is achieved for six distinct initial states. Besides being of fundamental interest, our result represents an important step towards a global quantum network. Moreover, the high-frequency and high-accuracy acquiring, pointing and tracking (APT) technique developed in our experiment can be directly utilized for future satellite-based quantum communication.

PACS numbers:

The application of quantum teleportation [1] has led to the discovery of seminal quantum information processing protocols, such as large-scale quantum communication [10] and linear optical quantum computing [11, 12]. Since quantum teleportation was first demonstrated with entangled photons in 1997 [2], photonic qubits have become very promising for the physical implementation of quantum information processing. Later, various developments have been achieved, including the demonstration of entanglement swapping [13], open-destination teleportation [14] and teleportation of two-bit composite system [15].

In addition to demonstrations in the laboratory, “practical” quantum teleportation over distances of about one kilometer have been realized via fiber links [6, 7]. Longer distance quantum teleportation using fiber links is not feasible due to the huge losses in the optical fibers. Free-space links, first used for quantum key distribution [16, 17] in 2002, hold promise for long-distance quantum teleportation. Since absorptive losses in the fiber are not a problem, entanglement can be shared using free-space links over distances of hundreds of kilometers. Moreover, with the help of satellite, the distance can be orders of magnitude higher. Since then, various experiments with entangled photon pairs have been achieved [18–21]. Most recently, following a modified scheme [3], quantum teleportation over 16 km free-space links was demonstrated [8] with a single pair of entangled photons. However, in this experiment, the unknown quantum state must be prepared on one of the resource entangled qubits and

therefore cannot be presented independently.

In our experiment, we demonstrate quantum teleportation of an independent unknown state between two optical free-space links separated by 97 km with multi-photon entanglement, following the original scheme [1, 2]. An average fidelity of 80.4(9) % can be achieved for six distinct initial states over a 35-53 dB loss quantum channel. The successful quantum teleportation over such channel losses in combination with our high-frequency and high-accuracy APT technique show the feasibility of satellite-based ultra-long-distance quantum teleportation.

A schematic illustration of free-space quantum teleportation is shown in Fig. 1a. Alice has a photon in an unknown quantum state $|\chi\rangle_1 = \alpha|H\rangle + \beta|V\rangle$, where H (V) represents the horizontal (vertical) polarization. Alice wants to transfer the photon to Bob, who is at a distant location. To do so, Charlie first distributes an entangled photon pair 2 and 3, $|\Phi^+\rangle_{23} = (|H\rangle|H\rangle + |V\rangle|V\rangle)/\sqrt{2}$, to Alice and Bob, respectively. The combinative state of the three photons can be rewritten as

$$|\chi\rangle_1 \otimes |\Phi^+\rangle_{23} = \frac{1}{2} (|\Phi^+\rangle_{12}|\chi\rangle_3 + |\Phi^-\rangle_{12}(Z|\chi\rangle_3) + |\Psi^+\rangle_{12}(X|\chi\rangle_3) + |\Psi^-\rangle_{12}(XZ|\chi\rangle_3)), \quad (1)$$

where $|\Phi^\pm\rangle_{12} = (|H\rangle_1|H\rangle_2 \pm |V\rangle_1|V\rangle_2)/\sqrt{2}$, $|\Psi^\pm\rangle_{12} = (|H\rangle_1|V\rangle_2 \pm |V\rangle_1|H\rangle_2)/\sqrt{2}$ are the four Bell states, and Z , X are Pauli operators, which act as unitary transformations. Then, if Alice performs a joint Bell-state measurement (BSM) on her two photons, photon 3 is instantaneously projected into the four states $|\chi_3\rangle$, $Z|\chi_3\rangle$,

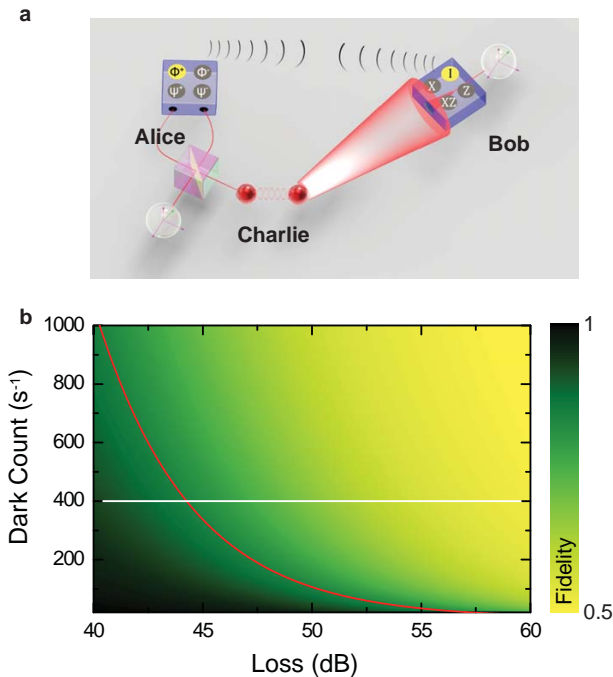


FIG. 1: Experimental scheme and calculated fidelity for practical free-space quantum teleportation. **a** Schematic drawing for practical free-space quantum teleportation. Charlie distributes an entangled pair of photons 2 and 3 to Alice and Bob, where Bob is at a distant location. Due to the finite size of the telescopes Bob and Charlie can use and the diffraction limit, Bob will receive the signal photon with very high loss. Alice then performs a joint Bell-state measurement (BSM) on the initial particle and one of the entangled photons from Charlie, projecting them onto an entangled state. After she has sent the result of her measurement as classical information to Bob, he can perform a unitary transformation (U) on his photon to obtain the initial state. **b** Calculated fidelity for ideal optics and an entangled photon source with the generation probability used in Ref. [24] as a function of total channel loss and the dark count on Bob's side. The red line shows the classical limit [25] of $2/3$. The white line shows the lowest dark count rate currently achieved via free-space link [21].

$X|\chi_3\rangle$ and $XZ|\chi_3\rangle$, respectively. Thus, after receiving the BSM result from Alice via a classical channel, Bob can apply the appropriate unitary transformation to convert the state of photon 3 to the initial state [1, 2].

Practically, the quantum channel between Charlie and Bob always has losses due to the finite size of the telescopes on both sides (see Fig. 1a). Typically, for an up-link of the ground station to a satellite, this loss can be up to 45 dB (calculated for 20 cm satellite optics at an orbit height of 500 km). The losses themselves only reduce the success probability of the teleportation. With perfect detectors and without background light, the channel losses would not be the limiting factor. However, because of the intrinsic dark counts by the detector and additional background from the environment, there is a

chance that a dark count produces an error each time a photon is lost. When the probability of a dark count becomes comparable to the probability that a photon is correctly detected, the signal-to-noise ratio tends to 0. In order to overcome this problem, one has two possibilities: increasing the brightness of the entangled photon source or reducing the dark count rate. The calculated fidelity as a function of dark count rate and channel loss is shown in Fig. 1b. One can see that even with ideal optics, it is not possible to demonstrate successful quantum teleportation under a 45 dB loss channel with the currently achieved lowest dark count rate of ~ 400 /s [21].

Experimentally, we start with an ultra-bright entangled photon source [9] based on type-II spontaneous parametric down-conversion [22] (SPDC). As shown in Fig. 2a, on Charlie's side (located at Gangcha next to Qinghai Lake, $37^\circ 16' 42.41''$ N $99^\circ 52' 59.88''$ E, altitude 3262 m), a femtosecond ultraviolet (UV) laser is created by frequency doubling of a pulsed laser (MIRA, central wavelength of 788 nm with a duration of 130 fs and a repetition rate of 76 MHz) with an LBO crystal (LiB_3O_5). The UV laser is further guided to pump a noncollinear type-II β -barium (BBO) crystal, resulting in a pair of polarization entangled photons in the state $|\Psi\rangle = (|H_oV_e\rangle + |V_eH_o\rangle)/\sqrt{2}$ with temporal and polarization information also entangled [9], where o and e indicate the polarization with respect to the pump. With an interferometric Bell-state synthesizer [9], we disentangle the temporal from the polarization information by guiding photons of different bandwidths through separate paths, resulting in the desired entangled photon source $|\Phi^+\rangle_{23} = (|HH\rangle + |VV\rangle)_{23}/\sqrt{2}$. Charlie then distributes the two photons 2 and 3 to Alice and Bob, respectively.

To prepare the unknown quantum state to be teleported, Alice uses the UV laser to pump a collinear BBO crystal which emits photons along the pumping light direction (see Fig. 2b). The generated photons are $|HV\rangle_{14}$, which are then split by a PBS after the pumping laser has been filtered out. A half wave plate (HWP) and a quarter wave plate (QWP) are applied in path 1 to create the initial state. Under a trigger on path 4, Alice creates the state she wants to teleport. Then, Alice performs a joint BSM on photon 1 and 2 by interfering them on a PBS and performing polarization analysis on the two outputs. The subsequent coincidence measurements can identify the $|\Phi^\pm\rangle$ Bell states in our experiment.

In the experiment, the power of the pulsed UV laser was about 1.3 W after frequency doubling. The observed average two-fold coincidence rate was 440 kHz with 3 nm filters in the e -ray path 2 and 8 nm filters in the o -ray path 3. The visibility of the entangled photon pair was about 91% in the $|H\rangle/|V\rangle$ basis and 90% in the $|+\rangle/|-\rangle$ basis, where $|\pm\rangle = 1/\sqrt{2}(|H\rangle \pm |V\rangle)$. The generation rate of the entangled photons was about 0.1, and the overall detection efficiency was 0.236 locally. The count rate

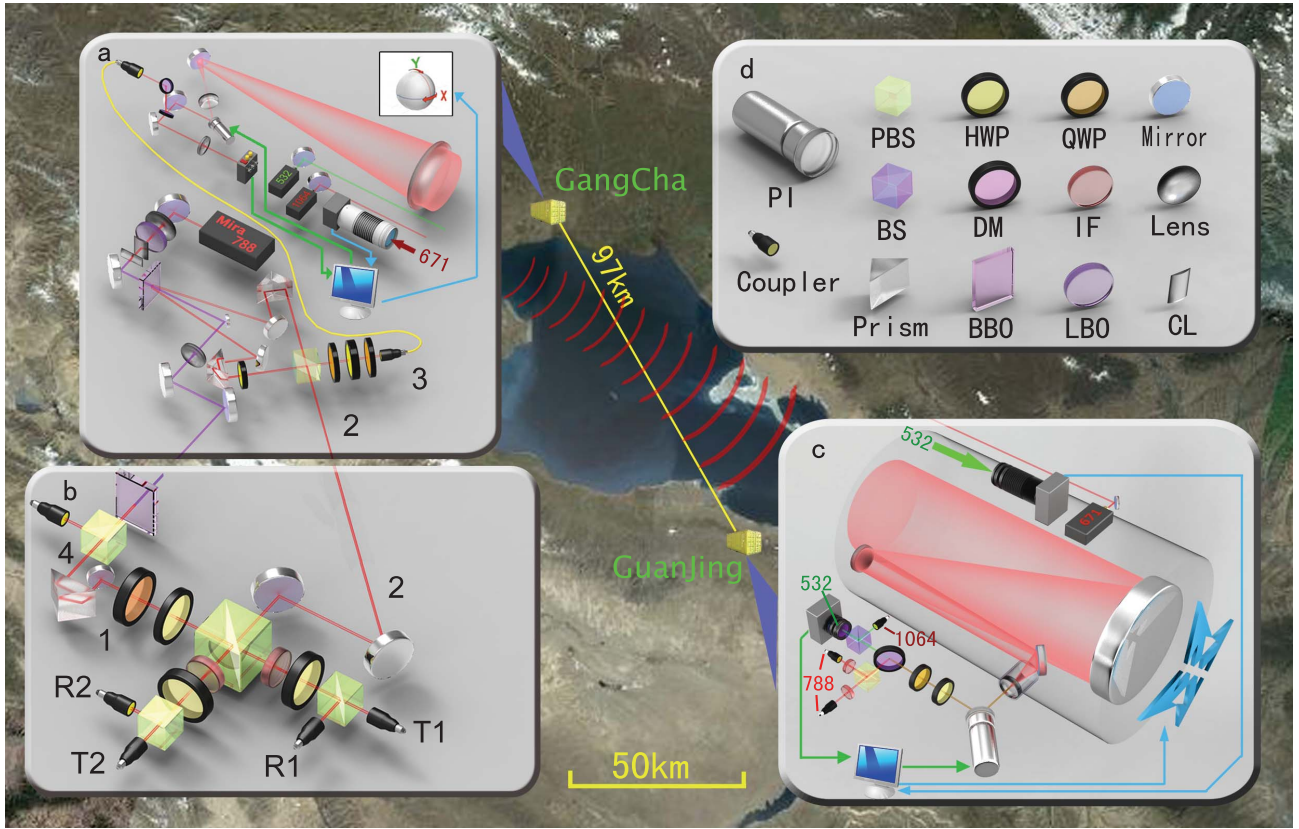


FIG. 2: Bird's-eye view and schematic diagram for free-space quantum teleportation. **a**, Entanglement generation and distribution on Charlie's side. A near infrared pulse (788 nm) is focused on an LBO crystal to create an ultraviolet laser pulse, which is then focused with two cylindrical lenses (CL) and passed through a 2 mm nonlinear BBO crystal. By an SPDC process, an entangled photon pair is created. An interferometric Bell-state synthesizer is utilized to disentangle the temporal from the polarization information [9]. While photon 2 is then directly sent to Alice for BSM, photon 3 is guided to a refractor telescope through a fiber and sent to Bob. A HWP sandwiched between two QWPs constitute the fiber polarization compensation. Coaxial with the telescope, there is a green laser (532 nm) for system tracking and a red laser (1064 nm) for synchronization. The green arrows indicate the fine tracking system which consists of a four-quadrant detector and a fast steering mirror driven by piezo ceramics (PI). The blue arrows indicate the coarse tracking system which consists of a wide-angle camera and a two-dimensional rotatable platform. **b**, Initial state preparation and BSM on Alice's side. Alice sends the UV laser through a collinear BBO, creating another photon pair which is later separated in path by a PBS. An HWP and a QWP is applied in path 1 to prepare the initial unknown quantum state to be teleported. Alice interferes the initial state 1 and the photon 2 from Charlie using another PBS. A 22.5° HWP and PBS is placed at both outputs for polarization analysis. A coincidence between detectors T1 and T2 (R2) or R1 and R2 (T2) indicates the incident state of $|\Phi^+\rangle$ ($|\Phi^-\rangle$). **c**, Polarization analysis on Bob's side. Bob receives photon 3 with a 400mm diameter off-axis reflecting telescope. A polarization analyzer is assembled at the telescope's exit, containing an HWP, a QWP, a PBS, and two multi-mode fiber-coupled SPCMs. Coaxial with the receiving telescope, there is another high-power beacon laser (671 nm) for system tracking. The blue and green arrows indicate the coarse and fine tracking system, respectively. **d**, Symbols used for the setup.

of photon pair $|HV\rangle_{14}$ generated by the collinear BBO crystal was 650 kHz, with the photon in path 1 (*e*-ray) filtered by an interference filter ($\Delta_{\text{FWHM}} = 3$ nm) and the photon in path 4 (*o*-ray) detected without filters. In the joint BSM, the observed visibility of interference for the photons overlapping on the PBS was 0.6. Finally, we observed about a 2 kHz counting rate for four-fold coincidence locally.

On the other hand, Charlie sends photon 3 with a compact transmitting system to Bob on the other side of Qinghai Lake, as shown in Fig. 2a. A 127mm f/7.5 ED

APO refractor telescope is employed as an optical transmitting antenna. By minimizing the color dispersion, we obtain superior sharpness and color correction. For near-diffraction-limited far-field divergence angles, we design systems to substantially reduce chromatic and spherical aberrations. Finally, the divergence angle of our compact quantum transmitter is about $20 \mu\text{rad}$.

As shown in Fig. 2c, Bob (GuanJing $36^\circ 32' 43.31''\text{N}$ $100^\circ 28' 9.81''\text{E}$, altitude 3682 m) receives photon 3 with a 400mm diameter off-axis reflecting telescope. An integrated measurement system, consisting of an HWP, a

QWP and a PBS, is assembled at the telescope's exit to measure any arbitrary state. Then, the photons are coupled in multi-mode fibers by a non-spherical lens. By selecting the appropriate fiber core and focal length, we compress the receiver field of view to $70 \mu\text{rad}$, which directly improves the system's signal-to-noise ratio. In front of the non-spherical lens, two band-pass filters ($\Delta_{\text{FWHM}} = 80 \text{ nm}$) and one narrow-band interference filter ($\Delta_{\text{FWHM}} = 10 \text{ nm}$) are used to reduce background noises (IF shown in Fig. 2c). Finally the photons are detected by the single-photon counting modules with ultra-low dark counts ($< 20 /\text{s}$). The noise that we observed, including the dark counts and ambient counts, is in total about $160 /\text{s}$ to $300 /\text{s}$. The noise mainly depends on the position of the moon.

In addition to the optical design previously mentioned, we also equip an APT system to account for effects due to ground settlement, mechanical deformation, atmospheric turbulence, etc. As shown in Fig. 2a, on the sender Charlie's side, coaxial with the entangled photon 3, there is a continuous green laser (532 nm, 200 mw, 1.5 mrad) for system tracking and a pulsed red laser (1064 nm, 10 kHz, 50 mw, $200 \mu\text{rad}$) for synchronization. On the receiver Bob's side, coaxial with the receiving telescope, there is a high-power beacon laser (671 nm, 2 w, $200 \mu\text{rad}$) for system tracking (Fig. 2c). When the optical link was established for the first time, Charlie achieved acquiring by Global Positioning System (GPS) coordinates and light guide. At the same time, he fired the beacon light (532 nm) pointing to the receiver Bob. Bob then achieved acquisition and fired another beacon light (671 nm) pointing back to Charlie.

The tracking system is then composed by a cascade close-loop control system (the blue and green arrows in Fig. 2a and 2c). On Charlie's side, the beacon laser from the receiver Bob is detected by a wide-angle camera. With a feedback loop, the coarse alignment of the entire optical system is achieved by the two-dimensional rotatable platform in both azimuth and elevation (blue arrows in Fig. 2a). Similarly, the fine tracking indicated by the green arrows is achieved by the four-quadrant detector and fast steering mirror driven by piezo ceramics. Furthermore, the fine tracking system shares the same optical path as the quantum channel and is later separated by a dichroic mirror (DM). Thus, a much higher tracking accuracy can be obtained. The closed-loop bandwidth of the fine tracking is more than 150 Hz, which is sufficient to overcome most of the atmospheric turbulence [23]. Finally with this designed system we get the tracking accuracy better than $3.5 \mu\text{rad}$ over 97km free-space link.

As indicated by the blue and green arrows in Fig. 2c, there are also coarse and fine tracking on the receiver Bob's side, by close-loop control via the telescope's own rack and piezo ceramics. Since the main purpose of the tracking system at the receiver is to reduce the low fre-

TABLE I: Fidelity of quantum teleportation over 97 km. The data collection was accumulated for 14400 s. The errors denote the statistical error, which is ± 1 standard deviation.

State	Fidelity
H	0.814 ± 0.031
V	0.886 ± 0.024
$+$	0.773 ± 0.031
$-$	0.781 ± 0.031
R	0.808 ± 0.026
L	0.760 ± 0.027

quency shaking due to ground settlement and passing vehicles, the closed loop bandwidth is about 10 Hz. The APT system is designed for tracking an arbitrarily moving object, which can be directly utilized for a satellite-based quantum communication experiment. In experiments between fixed locations, the first two steps, acquiring and pointing, do not need to be done every day.

In addition, we utilize Wireless Bridge for data transmission and classical communication between Alice and Bob. A high-accuracy Time-to-Digital Converter is used to independently record the arrival time of signals at both Alice's and Bob's station. Pulses per second with 10 ns jitter produced by the GPS are added to synchronize the starting time. With the help of the pulsed synchronization laser, we achieve a time synchronization accuracy of better than 1 ns.

After debugging the entire system, we measured the channel loss in the Qinghai Lake district over 97 km horizontal atmospheric transmission at near ground levels. The measured link efficiency was between 35 and 53 dB, in which 8 dB was due to the imperfect optics and finite collection efficiency and 8 to 12 dB was due to atmospheric loss. Further, the geometric attenuation due to beam spreading wider than the aperture of the receiver telescope was between 19 to 33dB, corresponding to the far-field spot size of between 3.5 and 17.9 m, depending on weather conditions. With the tracking accuracy of $3.5 \mu\text{rad}$ (0.34 m at the receiver), we got stable count rates for single photons. Finally, we obtained 1171 coincidences during an effective time of 14400 s. The average channel attenuation was about 44 dB, and the time accuracy was better than 1 ns. We selected linear polarization states $|H\rangle$, $|V\rangle$ and $|\pm\rangle = (|H\rangle \pm |V\rangle)/\sqrt{2}$, circular polarization states $|R\rangle = (|H\rangle + i|V\rangle)/\sqrt{2}$ and $|L\rangle = (|H\rangle - i|V\rangle)/\sqrt{2}$ as the initial states to be teleported. The final data results are shown in Table I. The experimental results for teleportation fidelity for different initial states range from 76% to 89%, with an overall average fidelity of 80%. The fidelities for the six teleported states were all well beyond the classical limit of $2/3$.

In summary, based on multi-photon entanglement, we experimentally realized free-space quantum teleportation over a 35–53 dB loss channel, and enhanced the transmis-

sion distance by an order of magnitude to 100 km. Our results show that even with high-loss ground to satellite uplink channels, quantum teleportation can be realized. Furthermore, our APT system can be used to track an arbitrarily moving object with high frequency and high accuracy, which is essential for future satellite-based ultra-long-distance quantum communication. We hope our experiment will boost the fundamental tests of the laws of quantum mechanics on a global scale.

We acknowledge insightful discussions with X.-S. Ma, R. Ursin and A. Zeilinger. This work has been supported by the NNSF of China, the CAS, the National Fundamental Research Program (under Grant No. 2011CB921300) and NSERC.

* These authors contributed equally to this work

- [1] C. H. Bennett *et al.*, Phys. Rev. Lett. **70**, 1895 (1993).
- [2] D. Bouwmeester *et al.*, Nature **390**, 575 (1997).
- [3] D. Boschi *et al.*, Phys. Rev. Lett. **80**, 1121 (1998).
- [4] M. Riebe *et al.*, Nature **429**, 734 (2004).
- [5] M. D. Barrett *et al.*, Nature **429**, 737 (2004).
- [6] I. Marcikic *et al.*, Nature **421**, 509 (2003).
- [7] R. Ursin *et al.*, Nature **430**, 849 (2004).
- [8] X.-M. Jin *et al.*, Nature Photonics **4**, 376 (2010).
- [9] X.-C. Yao *et al.*, arXiv: 1105.6318v1 [quant-ph] (2011).
- [10] H. J. Briegel, W. Dur, J. I. Cirac and P. Zoller, Phys. Rev. Lett. **81**, 5932 (1998).
- [11] D. Gottesman and I. L. Chuang, Nature **402**, 390 (1999).
- [12] E. Knill, R. Laflamme and G. J. Milburn, Nature **409**, 46 (2001).
- [13] J.-W. Pan, D. Bouwmeester, H. Weinfurter and A. Zeilinger, Phys. Rev. Lett. **80**, 3891 (1998).
- [14] Z. Zhao *et al.*, Nature **430**, 54 (2004).
- [15] Q. Zhang *et al.*, Nature Physics **2**, 678 (2006).
- [16] R. J. Hughes, J. E. Nordholt, D. Derkacs and C. G. Peterson, New J. Phys. **4**, 43 (2002).
- [17] C. Kurtsiefer *et al.*, Nature **419**, 450 (2002).
- [18] M. Aspelmeyer *et al.*, Science **301**, 621 (2003).
- [19] C.-Z. Peng *et al.*, Phys. Rev. Lett. **94**, 150501 (2005).
- [20] R. Ursin *et al.*, Nature Physics **3**, 481 (2007).
- [21] A. Fedrizzi *et al.*, Nature Physics **5**, 389 (2009).
- [22] P. G. Kwiat *et al.*, Phys. Rev. Lett. **75**, 4337 (1995).
- [23] J. W. Strohbehn, *Laser beam propagation in the atmosphere*. Berlin: Springer-Verlag (1978).
- [24] C.-Y. Lu *et al.*, Nature Physics **3**, 91 (2007).
- [25] S. Popescu, Phys. Rev. Lett. **72**, 797 (1994).